1-1990

Evolution of the Starspots in V478 Lyrae from 1980 to 1988

Douglas S. Hall
Vanderbilt University

Gregory W. Henry
Tennessee State University

James R. Sowell
Georgia State University

EVOLUTION OF THE STARSPOTS IN V478 LYRAE FROM 1980 TO 1988

DOUGLAS S. HALL
Dyer Observatory, Vanderbilt University, Nashville, Tennessee 37235

GREGORY W. HENRY
Center of Excellence in Information Systems, Tennessee State University, Nashville, Tennessee 37203

JAMES R. SOWELL
Center for High Angular Resolution Astronomy, Georgia State University, Atlanta, Georgia 30303
Received 6 March 1989; revised 3 October 1989

ABSTRACT

Differential *UBV* photometry of V478 Lyrae from 1980 to 1988 is presented and analyzed as 22 separate light curves, each spanning an average of a dozen rotation cycles. These are fit with a simple two-spot model, which does justice to the accuracy of the photometry: ± 0.010 mag for the 10 in. APT and ± 0.005 mag for the 16 in. APT. A given spot has an effective rotation period that can be considered constant; i.e., a single period represents epochs of minimum light to within their $\pm 0^{p}02$ uncertainties. The G8 V star rotates in approximate synchronism with the 2.13 day orbital period, but the different spots show different periods, ranging from 0.4% faster than synchronous to 0.5% slower than synchronous. Consideration of spot longitudes and spot areas shows that the beginning and end of several spots have been observed. Spots on V478 Lyr appear to have lifetimes on the order of several months to a year. The amplitude of the light loss produced by a spot can change by a factor of 2 within 20 days. In the only four determinate cases, it is shown that a spot came into existence at one of the two conjunctions, i.e., in the middle of the hemisphere facing (or opposing) the companion star. This provides additional support for the picture of a four-sector longitudinal structure, aligned with the major axis of the binary, which determines where magnetically active regions develop. The brightness of V478 Lyr at maximum, when presumably an unspotted hemisphere is being observed, is clearly variable, by 0.11 mag. These changes are as large as those produced when the two spots rotate into and out of view. V478 Lyr undergoes a shallow partial primary eclipse at the expected epoch (G8 V star behind) and no measurable secondary eclipse at the other conjunction. The solution of the primary eclipse, with assumed masses and radii for the two stars, yields an orbital inclination of $i = 82^{\circ}8$, a depth of 0.055 mag in V, and a duration of $D = 2.0$ hr.

I. INTRODUCTION

V478 Lyrae = HD 178450 is a fairly bright ($V = 7.7$ mag) SB1 with an orbital period of $2^{d}13$ and a chromospherically active G8 V star seen alone in the spectrum. The photometric variability was discovered by Henry (1981), who found an amplitude of 0.033 ± 0.005 mag in V, an apparent photometric period of $2^{d}185 \pm 0^{d}005$, and evidence of intrinsic changes in the light curve. The most recent and complete discussion of its characteristics as a spectroscopic binary and as a chromospherically active star is given by Fekel (1988). The unseen secondary star is probably an M2 or M3 dwarf, the distance is approximately 26 pc, and its age is somewhat younger than the Hyades. Strassmeier *et al.* (1989) analyzed the 1984–1986 seasons of photometry obtained with a 10 in. automatic telescope in Arizona (Hall, Kirkpatrick, and Seufert 1986), to see what periodicities and amplitudes showed up in a Fourier transform. They found the photometric period and the amplitude variable on a timescale shorter than one observing season.

In this paper we analyze the original 1980 photometry of Henry (1981), additional photometry obtained by Henry at Kitt Peak National Observatory and Cloudcroft Observatory in 1981 and 1982, the same 10 in. automatic telescope photometry analyzed by Strassmeier *et al.* (1989), additional photometry obtained with the same telescope during the 1987 season, and photometry obtained with Vanderbilt's 16 in. automatic telescope at Mount Hopkins (Hall 1989) during the 1988 season.

Our goal is to study in as much detail as possible the evolution of the dark regions on the photosphere of the G8 V star presumed to be causing the photometric variability. In the process, it will be seen, we find V478 Lyr to be an eclipsing binary, undergoing a shallow partial primary eclipse at the expected conjunction.

II. PHOTOMETRY

The 1980 photometry of Henry (1981) has been published. The subsequent 1981 and 1982 photometry of Henry is presented in Table I, where the first four entries are from Kitt Peak and the rest from Cloudcroft. The photometry from the 10 in. automatic telescope will appear in a paper by Boyd, Genet, Busby, Hall, and Strassmeier (1989). The photometry from Vanderbilt's 16 in. automatic telescope will be published elsewhere later.

Each datum is a mean of three comparisons between the variable and the comparison star HD 177878. The filters were selected to match the bandpasses of the *UBV* system. All photometry has been corrected for differential atmospheric extinction and transformed differentially to the standard photometric system.

The Kitt Peak and Cloudcroft photometry was in V only; the 10 in. photometry was in U, B, and V; and the 16 in. photometry was in B and V. Results from only the V-band photometry are presented. We repeated the analysis with the B-band photometry and found generally the same results. The U-band photometry was less useful because of the gener-

 0004-6256/90/010396-09$00.90

TABLE I. 1981 and 1982 photometry.

JD(hel.) 2440000 +	ΔV (mag)
4716.9100	+0.027
4717.9887	−0.074
4718.9084	+0.024
4719.8999	−0.070
4872.6219	−0.018
4873.6258	−0.020
4874.6185	−0.025
4877.6243	−0.024
4892.6402	−0.058
4893.6049	−0.005
5111.9687	−0.033
5115.9469	−0.037
5119.8946	−0.059
5120.8131	−0.006
5121.8274	−0.067
5122.9129	−0.010
5135.9437	0.000
5137.8862	+0.006
5141.9704	−0.013
5153.9392	−0.056
5196.7526	−0.008

ally larger observational errors. During the nights JD 2 446 218.5 to 2 446 246.5 inclusive, the yellow filter fell out of the 10 in. photometer; these data have been relegated to one data group. The photometry affected by the power supply malfunction during the interval ≈JD 2 446 400.0 to 2 446 550.0, as discussed by Strassmeier *et al.* (1989), was deleted; the problem must have started developing gradually about 75 days before that, as indicated by noticeably larger residuals from our light curve fits.

For analysis we divided the photometry into 22 data groups, listed in Table II. For each we give the number of three-measurement means, n, the mean Julian Date ⟨JD⟩, and the time span in days, Δt. Because the orbital (and photometric) period is so near 2.0 days, complete phase coverage within a group could be achieved only if $\Delta t > 15\%$ days. On the other hand, as we shall see, the light curve at times underwent significant changes (factor-of-2 changes in the amplitude, for example) on a timescale as short as a month.

TABLE II. The 22 data groups.

Data group	n	⟨JD⟩ 2440000 +	Δt (days)	k (mag/day)
1	17	4538.1	63	
2	10	4805.3	177	
3	11	5154.4	85	
4	23	5996.1	51	−0.0005
5	15	6141.0	36	
6	19	6176.9	30	
7	16	6207.8	20	
8	23	6232.3	27	
9	15	6265.9	38	
10	16	6297.2	21	
11	11	6318.7	14	
12	15	6340.7	26	
13	18	6372.1	31	−0.0008
14	13	6565.9	26	
15	14	6594.4	15	
16	23	6916.9	58	
17	13	6972.9	24	
18	18	7090.1	47	+0.0007
19	19	7283.4	13	
20	26	7303.4	27	
21	16	7323.9	12	
22	14	7424.7	18	

III. LIGHT CURVE FITTING WITH A TWO-SPOT MODEL

To combine the data within each group into a light curve required knowledge of the photometric period operating throughout the interval Δt. We experimented with period-finding techniques that relied on fits of the form

$$m = m_0' + A\cos(\theta - \theta_{\min}), \quad (1)$$

$$m = m_0' + B\cos[2(\theta - \theta_{\min})], \quad (2)$$

$$m = m_0' + A\cos(\theta - \theta_{\min}) + B\cos[2(\theta - \theta_{\min})] \quad (3)$$

where m is the differential magnitude, m_0' is the differential magnitude corresponding to mean brightness, θ is the phase angle computed with an assumed period, and $\theta_{\min}$ corresponds to minimum light. For most of the data groups the results were unsatisfactory. Generally, even with the optimum period, the residuals were considerably larger than the expected observational errors, and often the optimum periods found by the above three equations were very different.

Given our current understanding of the large starspot regions that occur in chromospherically active stars (Hall 1987), we need a light curve fitting scheme that can accommodate two spots of different area (producing different amounts of light loss), different longitude (not necessarily 180° apart), and different effective rotation periods (as would be expected by differential rotation if they were located at different stellar latitudes). Our model is fit with seven parameters: P_1 = photometric (rotational) period of spot 1, P_2 = photometric (rotational) period of spot 2, J_1 = JD of maximum light loss caused by spot 1, J_2 = JD of maximum light loss caused by spot 2, C_1 = maximum light loss, in magnitude units, produced by spot 1, C_2 = maximum light loss, in magnitude units, produced by spot 2, and m_0 = magnitude of an unspotted hemisphere. The loss of light is described by the "downward half" of a sinusoidal curve and hence is limited to a phase interval of 180°. In actuality a spot should affect the light curve over a phase range of 180° + $\Delta\theta$, where $\Delta\theta$ is the radius of the spot in degrees. In V478 Lyr, however, we find that the light loss is never more than 0.10 mag, implying spots less than about 30° in radius. Moreover, because of limb darkening and foreshortening, the influence on the light curve beyond the 180° range will be small. Spots at different latitudes will affect the light curve in similar ways because, fortunately, the orbital inclination is near 90° in this eclipsing binary.

This model is illustrated schematically in Fig. 1, for two spots separated by 135° in longitude and differing in area. It should be realized that this is not really a spot model but rather a light curve fitting scheme. As such, it does not determine spot latitudes, although J_1 and J_2 do specify the longitudes of the two spots. It does not determine spot areas or radii, although C_1 and C_2 should be proportional to the areas of the two spots if they are of nearly the same temperature.

The parameters resulting from optimum fits of the data groups are given in Table III. The actual solution was determined iteratively, with starting values for each parameter estimated by inspection of the light curve. Each parameter

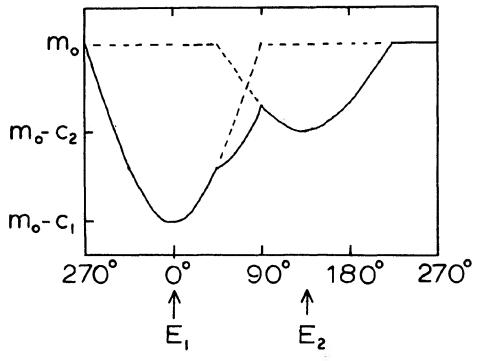

FIG. 1. Schematic light curve illustrating the two-spot modeling procedure. Spot 1 faces Earth at phase 0°, spot 2 at phase 135°; in other words, they are separated by 135° in stellar longitude. When neither spot is visible, the star has a magnitude m_0. Spot 1 causes the light to dim by the amount C_1, spot 2 by the amount C_2. The solid curve represents the combined effect of both spots, whereas the dashed curves illustrate the effects of each one separately. In this example, both spots have the same rotation period.

was allowed to vary over a suitable range with a suitably small incremental step. The optimum fit was that which yielded the minimum sum of the squares of the residuals. Because the solution procedure was iterative and did not involve matrix inversion, we could not use the curvature Hessian to demonstrate formally that a given solution was mathematically determinate. E_1 and E_2, the epochs of maximum light loss expressed in orbital cycles, have been computed with the ephemeris

$$\text{JD(conj.)} = 2\,445\,940.334 + 2^d130514\,E. \quad (4)$$

Here the time of conjunction (G8 V star behind) has been computed by adding a quarter-cycle to the time of maximum positive radial velocity given by Fekel (1988), and the period is the orbital period. The errors come from chi-square analysis. In three data groups (1, 10, and 15) the brightness changed monotonically over the interval Δt. This was corrected by adding a term of the form

$$k(\text{JD} - \langle\text{JD}\rangle).$$

For them the coefficient k, in units of magnitude per day, is given in the last column of Table II.

The rms residual from each of the fits is given in Table III. The residuals from data group 13 were largest because, we suspect, the previously mentioned power supply malfunction was beginning to develop. The residuals from the remaining data groups based on the 10 in. photometry (4–18) ranged from ± 0.005 to ± 0.013 mag, with an average of ± 0.009 mag. Strassmeier and Hall (1988) found external errors of ± 0.012 mag characteristic of that telescope, so we conclude that our fits have done justice to the observations. Residuals from fits to the last four light curves, which were obtained with the 16 in. telescope, proved to be even smaller: ± 0.004 or ± 0.006 mag.

The fits for three of the light curves (data groups 15, 17, and 20) are shown in Figs. 2–4.

No attempt was made to fit the two-spot model to the first three data groups, which contained relatively few data spread over relatively long intervals Δt. They were fit instead with Eq. (3). Their values of m_0', converted to differential magnitude at maximum brightness, are entered as m_0 in Table III. Those fits yielded the following best photometric periods: $2^d187 \pm 0^d006$, $2^d154 \pm 0^d002$, and $2^d131 \pm 0^d008$, respectively.

IV. PHOTOMETRIC PERIODS

Although the values of P_1 and P_2 yielding optimum fits to the data groups provided some indication of the photometric period of the two spots, a more precise measure can be derived from Fig. 5. Here we plot the fractional part of the spot phase versus whole-cycle number, both taken from E_1 and E_2 in Table III. If a line is fit through points belonging to the same spot, the slope of that line is the amount by which the spot's period is greater than (positive slope) or less than (negative slope) the orbital period.

There are two potential problems in such an approach. First, one must be sure that points belonging to the same spot are connected. Second, one must beware that proper cycle count has been maintained. The "instantaneous" periods P_1 and P_2 are helpful in countering this second problem. We have tentatively fit all points, except the pair from the very last light curve, with seven straight-line segments, identified as A–G. The corresponding periods, resulting from least-squares solutions, are given in Table IV. It is logical to infer that the beginning (or end) of a line segment signals the beginning (or end) of a spot as an organized area of diminished surface brightness.

We will see in the next section that consideration of gradual changes in the spot amplitudes suggests that two of the line segments in Fig. 5 (D and F) may have joined together an old spot and a new spot. Therefore, we have provided alternative solutions and entered these periods in Table IV as D′, D″, F′, and F″.

We are encouraged that the residuals from our straight-line fits (given as O − C in Table III) are extremely small and perfectly consistent with the formal uncertainties of the spot phases, i.e., the standard errors of the epochs of the spot minima (already given in Table III). For the 35 points fit by least squares the median residual is only $\pm 0^p018$, and the median standard error of the epochs E_1 and E_2 is also $\pm 0^p018$.

V. SPOT AMPLITUDES

A plot of spot amplitudes, taken from Table III, versus time can indicate how the area of each spot evolves with time. Those belonging to line segments A–G are plotted together in Fig. 6.

The amplitudes range from 0.000 ± 0.004 to 0.105 ± 0.006 mag, with the changes showing a tendency to be smooth and gradual rather than random or chaotic. In several cases a spot increases to a maximum and then decreases thereafter until it disappears, with no other points appearing later in time along that spot's line segment in Fig. 5. Gaps in the observational record prevent the evolution of some spots from being followed from beginning to end; we see them only increasing or decreasing in amplitude. In the case of two spots, D and F, we see the amplitude increase to a maximum and decrease to a minimum *twice*. This can be interpreted in two ways. Two different spots with coincidentally similar periods have been included in the same line segment, or there was one active region that experienced two episodes of spot formation and dissolution. Whichever interpretation we believe, we identify these two spots as D′ and

TABLE III. Parameters of the two-spot fits to the light curves.

data group	m_o (mag)	rms (mag)	spot	C (mag)	J 2440000+	E (cycles)	O-C (cycles)
1	-0.004	±0.007	-	-	-	-	-
2	-0.068	±0.015	-	-	-	-	-
3	-0.060	±0.007	-	-	-	-	-
4	-0.068	±0.012	A	0.060±0.005	5995.559±0.036	25.921±0.017	+0.008
			B	0.051±0.005	5997.136±0.026	26.661±0.012	+0.009
5	-0.070	±0.006	A	0.040±0.004	6139.798±0.037	93.622±0.018	-0.036
			B	0.054±0.004	6140.486±0.023	93.945±0.011	-0.035
6	-0.060	±0.008	A	0.025±0.005	6178.134±0.055	111.616±0.026	+0.029
			B	0.047±0.004	6177.001±0.034	111.084±0.016	+0.022
7	-0.038	±0.008		0.000±0.004			
			B	0.030±0.005	6204.785±0.032	124.125±0.015	-0.002
8	-	±0.012	D'	0.030±0.005	6233.318±0.042	137.518±0.020	+0.010
			B	0.050±0.006	6232.631±0.039	137.196±0.018	+0.006
9	-0.068	±0.011	D'	0.086±0.008	6265.206±0.020	152.485±0.009	-0.028
			C	0.044±0.007	6266.374±0.069	153.033±0.032	+0.010
10	-0.049	±0.010	D'	0.059±0.006	6297.299±0.040	167.549±0.019	+0.030
			C	0.033±0.006	6298.404±0.058	168.067±0.027	+0.006
11	-0.037	±0.010	C	0.035±0.010	6317.604±0.112	177.079±0.052	-0.007
			D'	0.015±0.008	6316.390±0.170	176.509±0.080	-0.012
12	-0.035	±0.013	C	0.042±0.008	6341.039±0.102	188.079±0.048	-0.036
			D"	0.036±0.008	6341.968±0.083	188.515±0.039	-0.045
13	-0.011	±0.016	C	0.023±0.011	6371.075±0.075	202.177±0.035	+0.027
			D"	0.048±0.008	6372.026±0.075	202.622±0.035	+0.050
14	-0.064	±0.011	E	0.057±0.007	6567.445±0.051	294.347±0.024	-0.009
			D"	0.049±0.010	6566.056±0.131	293.695±0.061	+0.007
15	-0.066	±0.005	E	0.072±0.003	6595.189±0.017	307.369±0.008	+0.025
			D"	0.061±0.004	6595.878±0.016	307.693±0.008	-0.012
16	-0.089	±0.009	E	0.097±0.004	6916.519±0.014	458.192±0.007	-0.027
			F'	0.035±0.004	6917.839±0.045	459.812±0.021	-0.030
17	-0.074	±0.008	E	0.105±0.006	6973.996±0.014	485.170±0.006	-0.028
			F'	0.042±0.005	6975.392±0.038	485.825±0.018	+0.045
18	-0.038	±0.010	E	0.065±0.007	7086.960±0.029	538.192±0.014	+0.038
			F"	0.015±0.005	7085.811±0.100	537.653±0.047	-0.016
19	-0.095	±0.006	G	0.067±0.004	7282.335±0.019	629.895±0.009	+0.005
			F"	0.073±0.004	7283.266±0.020	630.332±0.010	-0.009
20	-0.087	±0.006	G	0.050±0.003	7308.007±0.015	641.945±0.007	-0.014
			F"	0.046±0.002	7308.912±0.020	642.370±0.010	+0.027
21	-0.076	±0.004	G	0.044±0.002	7320.914±0.017	648.003±0.008	+0.010
			F"	0.026±0.002	7321.604±0.032	648.327±0.015	-0.018
22	-0.077	±0.004	-	0.065±0.002	7424.103±0.015	696.437±0.007	-
			-	0.032±0.003	7424.758±0.024	696.744±0.012	-

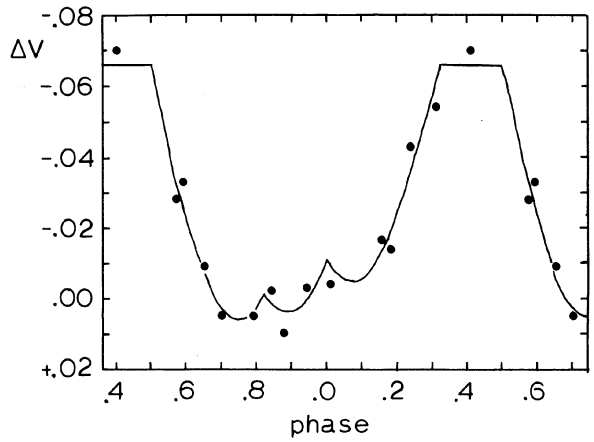

FIG. 2. Light curve of data group 15. The solid curve is the two-spot fit. Spot E faces Earth at JD 2.446 595.189 and has an amplitude of $C = 0.072$ mag. Spot D″ faces Earth at JD 2 446 595.878 and has an amplitude of $C = 0.061$ mag. Their longitude separation is only 116°. The rms deviation of the points from the curve is ± 0.005 mag. In this case, both spots had the same rotation period: $P = 2.13$ days.

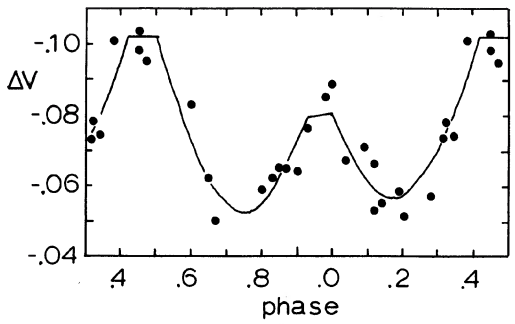

FIG. 4. Light curve of data group 20. The solid curve is the two-spot fit. Spot G faces Earth at JD 2 447 308.007 and has an amplitude of $C = 0.050$ mag. Spot F″ faces Earth at JD 2,447,308.912 and has an amplitude of $C = 0.046$ mag. Their longitude separation is 153°. The rms deviation of the points from the curve is ± 0.006 mag. In this case, both spots had the same rotation period: $P = 2.14$ days.

D″, and F′ and F″. The data group at E = 138 was obtained when the yellow filter had fallen out and the effective wavelength of the bandpass was approximately 4000 Å. The two amplitudes entered in Table III are those based on a fit of the *B*-band light curve. Because amplitudes in the *B* averaged about 25% larger than those in the *V*, we have plotted 0.040 and 0.024 mag in Fig. 6.

To estimate the beginning and end of each spot, we used the following criteria. If the rise to maximum amplitude or fall to minimum amplitude was steep, we extrapolated to zero amplitude. In some cases we adopted the epoch of the immediately preceding or immediately following light curve, in which a different spot was dominant. In other cases we could place only a limit on the beginning or end, because of the aforementioned gaps in the observational coverage.

These estimates are summarized in Table V. The implied spot lifetimes range from about 50 orbital cycles (3.5 months) to longer than 336 cycles (2.0 yr). The coverage of this longest-lived spot (E) included one 0.8 yr gap that

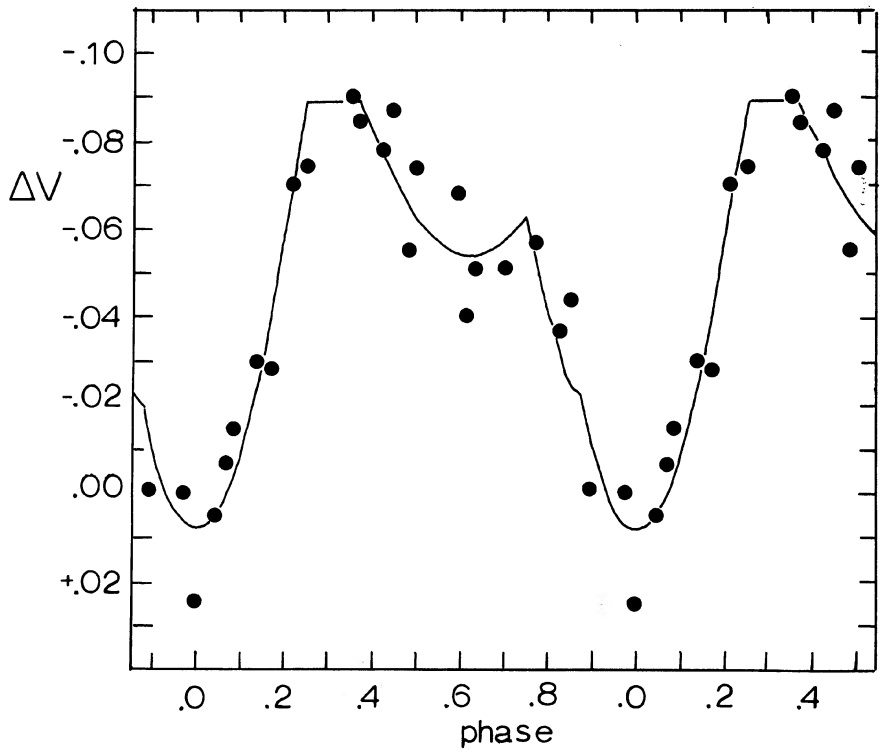

FIG. 3. Light curve of data group 17. The solid curve is the two-spot fit. Spot E faces Earth at JD 2.446 973.996 and has an amplitude of $C = 0.102$ mag. Spot F′ faces Earth at JD 2 446 975.392 and has an amplitude of $C = 0.042$ mag. Their longitude separation is 124°. The rms deviation of the points from the curve is ± 0.008 mag. In this case, both spots had the same rotation period: $P = 2.13$ days.

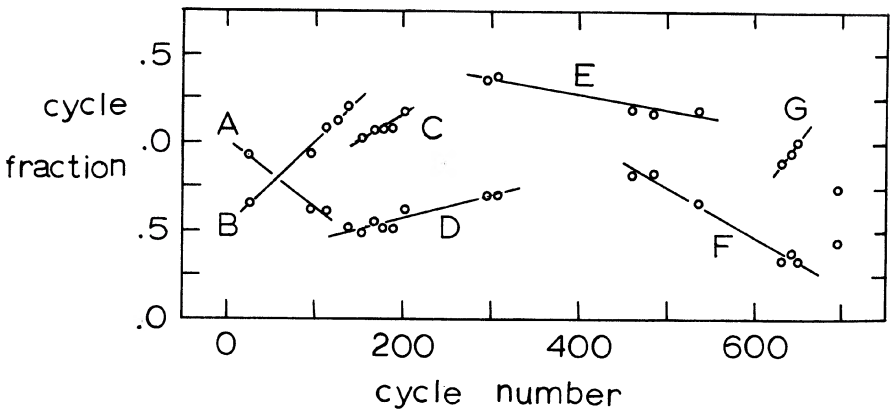

FIG. 5. Migration curves for the spots on the G8 V star in V478 Lyrae. The abscissa is orbital cycle number computed with the ephemeris in Eq. (4) and the ordinate is the fractional part, both taken from E in Table III. Points connected with the same straight-line segment belong to the same spot, identified as A–G. A negative slope means that the spot had a rotation period faster than synchronous, i.e., faster than $2^d.130\ 514$, and vice versa for positive slopes. The periods resulting from linear least-squares solutions are given in Table IV. The diameter of each point represents the average error bar.

might have concealed the end of one spot and the beginning of another. Even so, we see other spots with lifetimes longer than 8 or 9 months.

VI. PREFERRED LONGITUDES

It has been suggested that stars have a four-sector longitudinal structure and that magnetically active regions develop preferentially within two opposing sectors (Eaton and Hall 1979; Olah *et al.* 1986; Zeilik *et al.* 1988). Additionally it has been suggested that the sector structure is aligned with the line of centers if the chromospherically active star is in a binary system. Therefore it is of interest to examine the longitude at which the various spots on the G8 V star in V478 Lyr first appeared.

To do this we simply note the value of the orbital phase at the epoch of spot beginning. Since each spot has its own effective rotation period, differing from the oribital period, it migrates away from its point of origin. For each spot we use the parameters of the least-squares fits, seen in Fig. 5 and listed in Table IV, to extrapolate to the epoch of spot beginning, given in Table V. The results from four spots are given in Table VI. Nothing useful could be learned about the others because the epoch of their beginnings was not known with sufficient precision. The four cases in Table VI fall at one conjunction or the other, with residuals of -0.7, 0.0, $+1.0$, and -1.7 standard errors.

VII. VARIABILITY AT MAXIMUM

The values of m_0, taken from Table III, are plotted in Fig. 7. For each of the three data groups where a secular change in brightness was observed (4, 13, and 18) three points have been plotted instead of one. We see that the brightness of the supposedly unspotted hemisphere has not remained constant. The total range covered over the nine years was 0.11 mag, almost exactly (coincidentally?) equal to the light loss caused by the largest spot, in data group 17 in 1987.5.

We can offer no convincing explanation for these changes in brightness, although we considered several. Most puzzling were the three epochs (around cycle numbers -660, $+200$, and $+520$) when the brightness faded rather suddenly but briefly. The fading is not apparently periodic in any simple way. We looked for but found no consistent correlation with spot beginnings, spot endings, spot areas, spot separations, or spot periods.

TABLE IV. Spot rotation periods.

Spot	Period (days)
A	2.1224 ± 0.0016
B	2.1409 ± 0.0006
C	2.1360 ± 0.0016
D	2.1332 ± 0.0004
D′	2.1314 ± 0.0022
D″	2.1332 ± 0.0010
E	2.1287 ± 0.0003
F	2.1245 ± 0.0005
F′	2.1259 ± 0.0021
F″	2.1309 ± 0.0055
G	2.1426 ± 0.0029

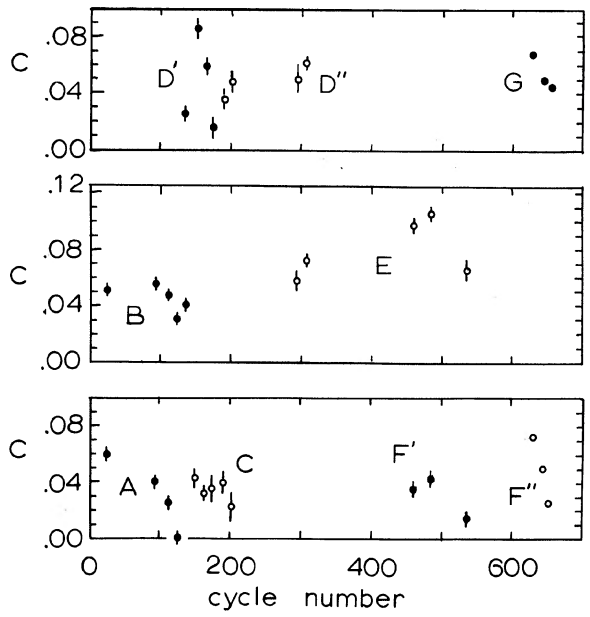

FIG. 6. Amplitudes of the various spots as a function of time, taken from *C* in Table III. Points belonging to the same spot have the same symbol; for example, closed circles for spot A, open circles for spot C, etc. The error bars for spots F″ and G are no bigger than their symbols.

TABLE V. Spot lifetimes.

Spot	Beginning (cycle)	Max. ampl. (cycle)	End (cycle)	Lifetime (cycles)
A	<26.2 (1)	26.2:	124.4 (2)	>98
B	<26.9 (1)	94.2	153.0 (4)	>126
C	137.6 (3)	153.3	218.8 (4)	81
D′	129.6 (2)	152.7	179.8 (2)	50
D″	177.0 (3)	307.9:	>307.9 (1)	>131
E	202.6 (3)	485.4	>538.4 (1)	>336
F′	<459.1 (1)	486.1	566.5 (2)	>107
F″	<630.6 (1)	630.6:	656.4 (2)	>26
G	<630.1 (1)	630.1:	696.8 (4)	>67

Notes to Table V
(1) Limited by gap in observational data.
(2) Extrapolation to zero amplitude.
(3) Epoch of previous spot.
(4) Epoch of following spot.

TABLE VI. Phase of spot beginning.

Spot	Phase
C	0.98 ± 0.03
D′	0.50 ± 0.04
D″	0.54 ± 0.04
E	0.43 ± 0.04

VIII. ECLIPSES

During our analysis we noticed that measurements taken at one of the conjunctions (G8 V star behind) were showing large residuals of the same sign in most of our light curve fits. We removed those in the phase range 0P98–0P02 as computed with the orbital ephemeris in Eq. (4). Later we computed residuals of those measurements, as well as of all measurements, with respect to the final parameters given in Table III.

Figures 8 and 9 are plots of those residuals versus phase in the vicinity of suspected primary eclipse (0P95–0P05) and suspected secondary eclipse (0P45–0P55). Points expected *a priori* to be of low weight have different symbols. These include residuals from fits of data groups 1–3 using Eq. (3) rather than our two-spot model and residuals from data group 13, which was affected by the power supply malfunction.

A primary eclipse is clearly present in Fig. 8. Of the 14 points between 0P98 and 0P02, 13 have residuals that make them too faint. The depth at mideclipse is around 0.05 mag in V. The duration, from first to fourth contact, is around $D = 0^{P}04 = 2.0$ hr. On the other hand, no secondary eclipse is evident in Fig. 9. The average of the seven residuals between 0P49 and 0P51 is faint by 0.002 ± 0.002 mag, which is not significantly different from zero.

To solve this shallow, obviously partial eclipse for the orbital inclination, we take the following absolute dimensions from Fekel (1988): $0.93\mathcal{M}_{\odot}$, $0.98R_{\odot}$ for the G8 V star and $0.25\mathcal{M}_{\odot}$, $0.30R_{\odot}$ for the M-type dwarf. Fekel had assumed $0.3\mathcal{M}_{\odot}$ for the M-type dwarf because he believed the inclination was around 67°, but we know now that it is closer to 90°. These dimensions yield $a = 0.034$ AU $= 7.33R_{\odot}$, and thus $r_h = 0.134$ and $r_c = 0.041$. Further assuming $x_h = 0.6$ for the limb-darkening coefficient of the G8 V star and $L_h = 1.0$, we find that an inclination of $i = 82^{\circ}8$ best fits all of the residuals. The solid curve in Fig. 8 represents this solution. The depth at midprimary eclipse is 0.055 mag in V and the external contact is at $\theta_e = 0^{P}196$, corresponding to $D = 2.0$ hr.

This solution depends, of course, on the various assumed parameters. Adopting radii and masses different by 10% would change the resulting inclination by about a half-degree. Our assumption of $L_h = 1.0$ is relatively good. The ratio of the surface brightnesses implied by the observed depth of secondary eclipse, $J_c/J_h = 0.036 \pm 0.040$, and the ratio of the radii, $k = 0.3$, dictate $L_h = 0.997 \pm 0.004$.

From the spectroscopic orbital parameters, Fekel (1988) had estimated $i = 67^{\circ} \pm 12^{\circ}$, but his upper limit was based on the assumption that eclipses *did not occur* in V478 Lyr. Thus he actually limited the inclination to the range $55^{\circ} < i < 90^{\circ}$, which is entirely consistent with our value of $i = 82^{\circ}8$.

IX. CONCLUSIONS

The G8 V star in V478 Lyr is rotating in approximate synchronism with its 2.13 day orbital period. The various light curves, each spanning an average of a month (a dozen rotation cycles), can be fit with a simple two-spot model. These fits do justice to the accuracy inherent in the photometry: ± 0.010 mag for the 10 in. automatic telescope and

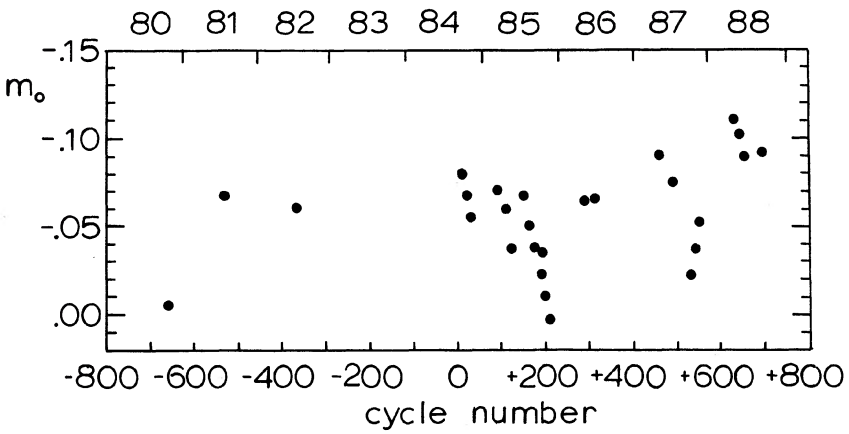

FIG. 7. Behavior of m_0 with time, where m_0 is the magnitude of a supposedly unspotted hemisphere. It varies over a range of 0.11 mag. The uncertainty of each point is no bigger than each circle.

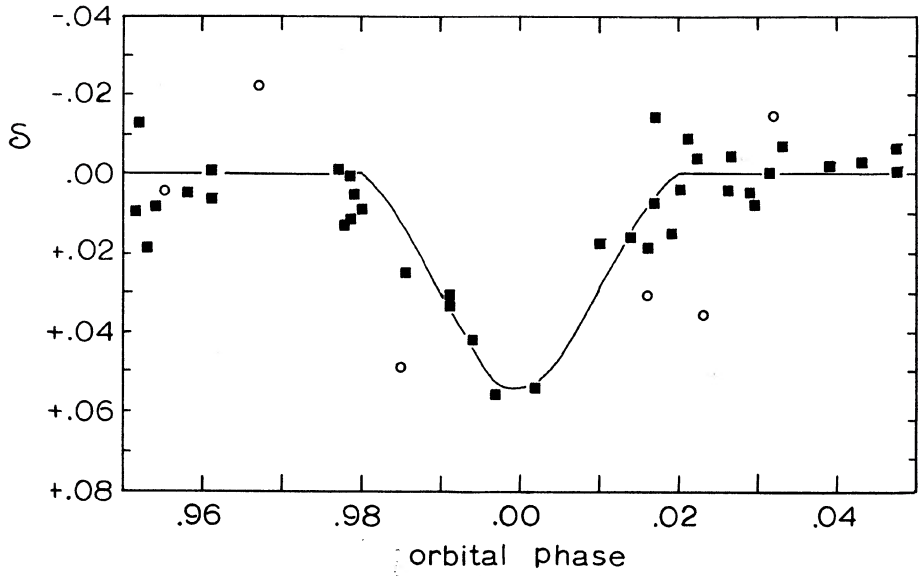

FIG. 8. Light curve in the vicinity of conjunction (G8 V star behind). Phases are computed with Eq. (4) and the ordinate δ is the residual from the two-spot model fits to the different data groups. The open circles have relatively low weight. The solid curve represents the solution discussed in Sec. VIII. The inclination is $i = 82°.8$, the depth is 0.055 mag in V, and the duration from first to fourth contact is 2.0 hr.

$\pm$ 0.005 mag for the 16 in. automatic telescope.

A given spot has an effective rotation period that can be considered strictly constant; i.e., a constant period represents epochs of minimum light to within their $\pm$ 0^{p}.02 uncertainties. The different spots show different periods, ranging from 0.4% faster than synchronous to 0.5% slower than synchronous, presumably as a result of differential rotation. (Periods derived from the early Henry data showed a wider range, the largest being 2^{d}.187, but it is not certain that those periods can be interpreted meaningfully, even as a mean of two spot periods.) Consideration of spot longitudes (Fig. 5) and spot areas (Fig. 6) shows that the beginning and end of several spots has been observed. Spots on V478 Lyr appear to have lifetimes (Table V) on the order of several months to a year. The amplitude of the light loss produced by a spot (and hence the area and/or darkness of a spot) can change by a factor of 2 within 20 days.

In the only four determinate cases, it can be shown (Table VI) that a spot came into existence at one of the two conjunctions, i.e., in the middle of the hemisphere facing (or opposing) the companion star. This provides additional support for the picture of a four-sector longitudinal structure, aligned with the major axis of the binary, which determines where magnetically active regions develop. The spotted star in a very close binary, such as the short-period RS CVn binaries or the W UMa binaries (Hall 1976), should have its differential rotation greatly diminished by the very strong tidal locking. In such a star an active region should live and die not far from its place of origin, i.e., spend its entire lifetime within its preferred sector. We suggest this as an explanation of the distribution of spot longitudes observed by Zeilik *et al.* (1988) in the short-period RS CVn binary SV Cam ($P = 0^{d}.59, r = 0.326$). In a not so close binary like V478 Lyr ($P = 2^{d}.13, r = 0.134$), with significant differential rotation, a spot will migrate away from the longitude of its origin. This makes it much more difficult to investigate the phenomenon of sector structure, because one must be able to determine the longitude of a spot at the epoch of its origin, not just at an arbitrary epoch or average of several epochs.

The brightness of V478 Lyr at maximum, when presumably an unspotted hemisphere is being observed, is clearly variable. These changes are as large as those produced when

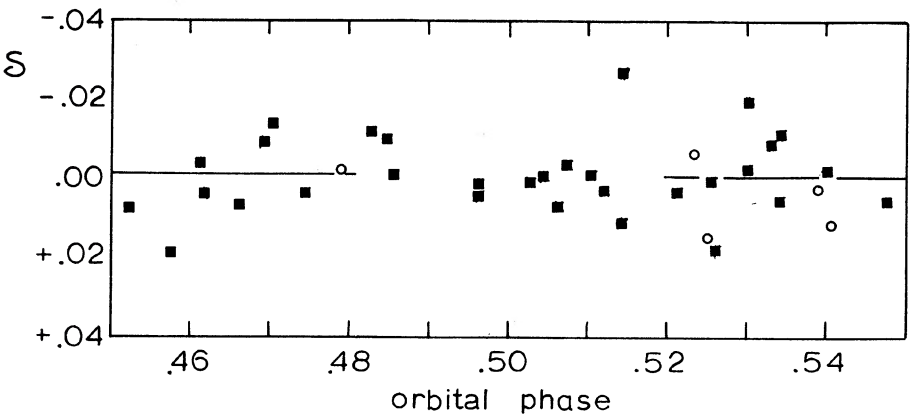

FIG. 9. Light curve in the vicinity of the other conjunction. The solid curve at $\delta = 0.00$ mag, representing the light level outside eclipse, has been left open between the first and fourth contacts as computed from the solution of the primary eclipse in Fig. 8. The depth of the secondary eclipse is immeasurably small.

the two spots rotate into and out of view, but we can offer no useful explanation.

V478 Lyr undergoes a shallow partial primary eclipse at the expected epoch (G8 V star behind) and no measurable secondary eclipse at the other conjunction. The solution of the primary eclipse, with assumed masses and radii for the two stars, yields an orbital inclination of $i = 82.^{\circ}8$.

We thank Mary D. Morton for assistance with many of the calculations. A research grant from the National Science Foundation (AST 84-14594) made construction of the Vanderbilt 16 in. automatic telescope possible and a research grant from the National Aeronautics and Space Administration (NAG 8-111) has made its continuing operation possible.

REFERENCES

Boyd, L. J., Genet, R. M., Busby, M. R., Hall, D. S., and Strassmeier, K. G. (1989). Astrophys. J. Suppl. (submitted).
Eaton, J. A., and Hall, D. S. (1979). Astrophys. J. **227**, 907.
Fekel, F. C. (1988). Astron. J. **95**, 215.
Hall, D. S. (1976). In *Multiple Periodic Variable Stars*, edited by W. S. Fitch (Reidel, Dordrecht), p. 287.
Hall, D. S. (1987). Publ. Astron. Inst. Czech. **70**, 77.
Hall, D. S. (1989). In *Automatic Small Telescopes*, edited by D. S. Hayes and R. M. Genet (Fairborn, Mesa, AZ), p. 65.
Hall, D. S., Kirkpatrick, J. D., and Seufert, E. R. (1986). IAPPP Commun. No. **25**, 32.
Henry, G. W. (1981). Inf. Bull. Var. Stars No. 1928.
Olah, K., Hall, D. S., Boyd, L. J., Genet, R. M., Fried, R. E., Lines, R. D., Lines, H. C., Louth, H., Miles, R., Nielsen, P., Stelzer, H. J., Troeger, J. C., and Wasson, N. F. (1986). Astrophys. Lett. **25**, 133.
Strassmeier, K. G., and Hall, D. S. (1988). Astrophys. J. Suppl. **67**, 439.
Strassmeier, K. G., Hall, D. S., Boyd, L. J., and Genet, R. M. (1989). Astrophys. J. Suppl. **69**, 141.
Zeilik, M., DeBlasi, C., and Rhodes, M. (1988). Astrophys. J. **332**, 293.